Controlled Synthesis and Assembly of FePt Nanoparticles

Shouheng Sun,*† Simone Anders,‡ Thomas Thomson,‡ J. E. E. Baglin,‡ Mike F. Toney,‡,§ Hendrik F. Hamann,† C. B. Murray,† and Bruce D. Terris‡

IBM T. J. Watson Research Center, Yorktown Heights, New York 10598, and IBM Almaden Research Center, 650 Harry Road, San Jose, California 95120

Received: October 26, 2002; In Final Form: February 19, 2003

Monodisperse 4 nm FePt magnetic nanoparticles were synthesized by superhydride reduction of $FeCl_2$ and $Pt(acac)_2$ at high temperature, and thin assemblies of FePt nanoparticles with controlled thickness were formed via polymer mediated self-assembly. Adding superhydride ($LiBEt_3H$) to the phenyl ether solution of $FeCl_2$ and $Pt(acac)_2$ in the presence of oleic acid, oleylamine, and 1,2-hexadecanediol at 200 °C, followed by refluxing at 263 °C, led to monodisperse 4 nm FePt nanoparticles. The initial molar ratio of the metal precursors was retained during the synthesis, and the final FePt composition of the particles was readily tuned. Alternately, adsorbing a layer of polyethylenimine (PEI) and the FePt nanoparticles onto a solid substrate resulted in nanoparticle assemblies with tunable thickness. Chemical analysis of the assemblies revealed that more iron oxide was present in the thinner assemblies annealed at lower temperature or for shorter time. Thermal annealing induced the internal particle structure change from chemically disordered fcc to chemically ordered fct and transformed the thin assembly from superparamagnetic to ferromagnetic. This controlled synthesis and assembly can be used to fabricate FePt nanoparticle-based functional devices for future nanomagnetic applications.

Introduction

Controlled synthesis and assembly of small hard magnetic particles has attracted great interest because of their potential applications in ultrahigh-density magnetic recording,[1,2] highly sensitive magnetic sensors,[3,4] and advanced nanocomposite permanent magnets.[5] The hard magnetic FePt materials are excellent candidates for these particle-based applications. They are more chemically stable than other well-known hard magnetic materials such as CoSm, NdFeB, and have very high magnetocrystalline anisotropy, K_u. In an ordered intermetallic phase, K_u can reach values as high as 10^8 erg/cm^3,[6] indicating that the magnetic anisotropy energy K_uV of a single 3 nm diameter magnetic grain (V is the magnetic grain volume) is much larger than the thermal energy k_BT (k_B is the Boltzman's constant and T is the temperature) at ambient temperatures. Recent advances in magnetic recording technology have indicated that, if self-assembled in a tightly packed, exchange-decoupled array with controlled magnetic easy axis direction, these FePt nanoparticles could support high-density magnetization reversal transitions and would be a candidate for future ultrahigh density data storage media, with potentially one bit per particle.[2,7]

To use self-organized FePt nanoparticles for magnetic recording applications, a practical route to monodisperse ferromagnetic FePt nanoparticles and nanoparticle assemblies with controlled assembly thickness and surface roughness is needed. Solution-phase-based high-temperature decomposition of $Fe(CO)_5$ and reduction of platinum acetylacetonate, $Pt(acac)_2$, was recently developed to make monodisperse FePt nanoparticles[8−11] and has been demonstrated to be a general approach to other multicomponent nanoparticles, including binary FeMo,[12] and ternary CoFePt[13] and AgFePt[14] nanoparticles. However, for future practical applications, several issues regarding this decomposition/reduction process need to be addressed. $Fe(CO)_5$ is volatile and is thermally unstable, gradually releasing CO and Fe at ambient temperature, rendering $Fe(CO)_5$ a well-known toxic chemical. The high-temperature condition of the synthesis needs an excess of $Fe(CO)_5$. A correlation between the molar ratio of $Fe(CO)_5/Pt(acac)_2$ and FePt composition always needs to be established in order to determine the final composition of the particles.[9] Furthermore, for nanoparticles to store magnetic information at density over 100 Gbit/in^2, they have to be arranged in a smooth thin assembly with a thickness of ∼10 nm.[15] It is therefore desired that the synthesis use less toxic metal precursors, and that the initial molar ratio of metal precursors be carried over to the final product, and that the nanoparticles be assembled with controlled assembly thickness.

We report a simple chemical process of synthesizing FePt nanoparticles by reduction of $FeCl_2$ and $Pt(acac)_2$ at 200 °C, followed by refluxing at 263 °C. The particle growth is self-limited and 4 nm FePt nanoparticles are readily separated. The initial molar ratio of the metal precursors is carried over to the final product, and the FePt composition is easily tuned. We further demonstrate that alternate adsorption of polyethylenimine (PEI) and FePt nanoparticles on a HO-terminated surface via surface ligand exchange leads to 4 nm FePt nanoparticle assemblies with controlled thickness. Thermal annealing is applied to control structural and magnetic properties of the assemblies. This controlled synthesis and assembly of FePt nanoparticles offers a convenient route for future fabrication of FePt nanoparticle-based devices.

Experimental Section

The synthesis was carried out using standard airless procedures and commercially available reagents. Absolute ethanol,

* To whom correspondence should be addressed. E-mail: ssun@us.ibm.com.
† IBM T. J. Watson Research Center.
‡ IBM Almaden Research Center.
§ Present address: Stanford Synchrotron Radiation Laboratory, Stanford Linear Accelerator Center, 2575 Sand Hill Road, Menlo Park, CA 94025.

10.1021/jp027314o CCC: $25.00
Published on Web 05/14/2003

hexane, and chloroform were used as received. Tetrahydrofuran (THF) solution of superhydride ($LiBEt_3H$) (1M), phenyl ether (99%), 1,2-hexadecanediol (97%), oleic acid (90%), iron (II) chloride tetrahydrate ($FeCl_2 \cdot 4H_2O$), and polyethylenimine (water-free, average. M_w ca. 25000) were purchased from Aldrich Chemical Co. Oleylamine (>70%) was from Fluka, and platinum acetylacetonate, $Pt(acac)_2$, was from Strem Chemicals, Inc.

Synthesis of $Fe_{58}Pt_{42}$ Nanoparticles. $Pt(acac)_2$ (197 mg, 0.5 mmol), $FeCl_2 \cdot 4H_2O$ (139 mg, 0.70 mmol), 1,2-hexadecanediol (520 mg, 2 mmol), and phenyl ether (25 mL) were added under nitrogen atmosphere, into a flask equipped with a N_2 in/outlet, septa rubber, and a thermal probe. The mixture was heated to 100 °C for 10 min. Oleic acid (0.16 mL, 0.5 mmol) and oleylamine (0.17 mL, 0.5 mmol) were added, and the mixture was continuously heated to 200 °C for 20 min. $LiBEt_3H$ (1 M THF solution, 2.5 mL) was slowly dropped into the mixture over a duration of ~2 min. The black dispersion was stirred at 200 °C for 5 min under N_2 to remove low boiling solvent and under a blanket of N_2 was heated to reflux at 263 °C for 20 min. The heating source was removed, and the black reaction mixture was cooled to room temperature. Ethanol (40 mL) was then added under ambient condition. The black product was precipitated and separated by centrifugation (6000 rpm, 10 min). The yellow-brown supernatant was discarded and the black product was dispersed in hexane (~20 mL) in the presence of oleic acid (~0.05 mL) and oleylamine (~0.02 mL). Any undissolved material was removed by centrifugation (6000 rpm, 10 min). The product was then precipitated out by adding ethanol (~20 mL) and separated with centrifugation (6000 rpm, 10 min). It was once again dispersed in hexane in the presence of oleic acid and oleylamine, precipitated out by adding ethanol and separated with centrifugation. The product, $Fe_{58}Pt_{42}$ nanoparticles, was re-dispersed in hexane solvent for further use.

Similarly, 0.61 mmol of $FeCl_2$ and 0.5 mmol $Pt(acac)_2$ led to $Fe_{55}Pt_{45}$ nanoparticles, and 0.5 mmol of $FeCl_2$ and 0.5 mmol $Pt(acac)_2$ to $Fe_{50}Pt_{50}$ nanoparticles.

Nanoparticle Assembly. A naturally oxidized silicon substrate was cleaned using ethanol and dried under a flow of N_2. The substrate was then immersed into the chloroform solution of PEI (~20 mg/mL) for about 30 s, withdrawn from the solution and dipped into ethanol solvent to wash off extra PEI on the substrate surface and dried. The PEI functionalized substrate was immersed into the hexane dispersion of FePt nanoparticles (10 mg/mL) for 30 s, withdrawn from the dispersion, rinsed with fresh hexane, and dried. This yielded one layer of PEI/FePt assembly. By repeating the coating of PEI and FePt, the multilayer of 4 nm FePt nanoparticle assembly was easily made.

Thermal Annealing of the FePt Nanoparticle Assemblies. The PEI/FePt assemblies were thermally annealed for further characterization. The annealing transforms the particle structure from the chemically disordered fcc phase to the chemically ordered fct phase, rendering FePt nanoparticles with desirable high magnetocrystalline anisotropy and ferromagnetism at room temperature.[8] Further, the annealing also results in the decomposition of the PEI and oleic acid/oleylamine left around FePt particles into carbonaceous matrix, yielding smooth FePt nanoparticle assemblies. The annealing was performed in an inert atmosphere (N_2 or He) or under $Ar + H_2(5\%)$ in a quartz tube at temperatures ranging from 400 to 800 °C and durations between 2 min and 2 h.

Nanoparticle Characterization. Fe and Pt elemental analyses of the as-synthesized FePt nanoparticle powders were performed on inductively coupled plasma−optic emission spectrometry (ICP−OES) at Galbraith Laboratories, Knoxville, TN. The particles were precipitated from their hexane dispersion by ethanol, washed with ethanol, and dried. Composition and thickness of the FePt nanoparticle assembly were determined by Rutherford backscattering spectrometry (RBS).

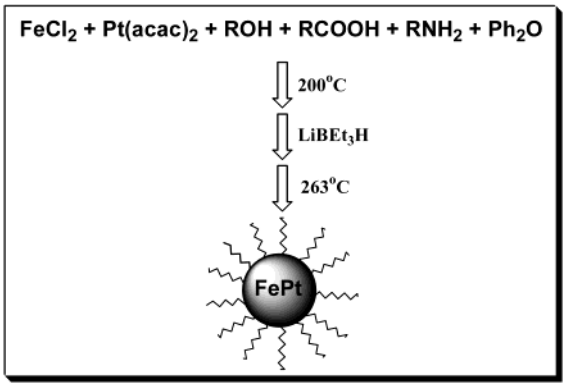

Figure 1. Schematic illustration of FePt nanoparticle synthesis by superhydride reduction of $FeCl_2$ and $Pt(acac)_2$ in the presence of oleic acid, oleylamine, and 1,2-hexadecanediol.

Samples for transmission electron microscopy (TEM) analysis were prepared by drying a hexane dispersion of FePt particles on amorphous carbon coated copper grids. Particle size was determined using a Philips CM 12 TEM (120 KV). The thin-layered PEI/FePt assembly was imaged using CM 12 TEM with the assembly on silicon oxide coated copper grids. The layered structure on naturally oxidized silicon (100) substrate was characterized by X-ray reflectivity measurements of the films. The measurements were conducted using Cu $K\alpha_1$ radiation from an 18 kW X-ray generator, monochromatized with flat Ge(111) crystal. The background (diffuse) scattering was subtracted from the raw data to yield the true specular reflectivity. A commercial atomic force microscope (AFM) was used for analysis of the surface morphology of the layered assembly (Digital Instruments, Nanoscope IIIa, Multimode).

The chemical nature of the films was studied using near edge X-ray absorption fine structure (NEXAFS) spectroscopy. The experiments were performed at the Advanced Light Source at beamline 7.3.1.1. that was equipped with a spherical grating monochromator and had an energy resolution of $E/\Delta E = 1800$. X-ray diffraction (XRD) measurements were performed in grazing incidence geometry at the National Synchrotron Light Source using beamline X20C. The diffracted beam was analyzed with 1 milliradian Soller slits, which provided a resolution much smaller than any of the diffraction peak widths.

Magnetic studies were carried out using a MPMS2 Quantum Design SQUID magnetometer with fields up to 5 T and temperatures from 5 to 350 K, and an Oxford instruments vibrating sample magnetometer with field up to 9 T at room temperature. Measurements were done on various layered FePt nanoparticle assemblies on thermally oxidized p-type silicon (100) substrates.

Results and Discussion

Synthesis Issues. As illustrated in Figure 1, the reduction of $FeCl_2$ and $Pt(acac)_2$ mixture by superhydride in the presence of oleic acid, oleylamine, and 1,2-hexadecanediol at 200 °C, followed by refluxing at 263 °C, led to monodisperse 4 nm FePt nanoparticles. Although the reduction was usually performed at 200 °C, experimental results show that superhydride could be added at any temperature in the range between 200 and 263

°C. Adding the reducing agent at lower temperature (<200 °C) did not yield high quality FePt nanoparticle materials.

Two metal precursors, $FeCl_2$ and $Pt(acac)_2$, were specifically chosen for this reduction process as they formed clear phenyl ether solution when mixed. Presumably, the mixing of $FeCl_2$ and $Pt(acac)_2$ resulted in an $FeCl_2-Pt(acac)_2$ intermediate that facilitated the formation of FePt nanoparticles under the current reaction condition. Other combinations of Fe salts, such as $FeCl_3$ and $Fe(acac)_3$, and Pt salts, such as $PtCl_2$ and K_2PtCl_4, did not yield good quality FePt nanoparticles. The $FeCl_2$ used in the reaction can be in either anhydrous state or hydrated state. If $FeCl_2 \cdot 4H_2O$ was used, the mixture was usually stirred at 200 °C under nitrogen for about 20 min before the reducing agent, superhydride, was added to the mixture.

Several different reducing agents have been tested for the reduction process. Metal naphthalides are very powerful reducing agents but are also difficult to store because of their extremely air- and moisture-sensitive nature. Polyalcohols, such as ethylene glycol and 1,2-hexanedecanediol, or other long chain alkyl alcohols are not a strong reducing agent for the $FeCl_2-Pt(acac)_2$ reduction. However the alkyl alcohol can act like a cosurfactant and help to generate FePt nanoparticles with better quality. Metal borohydrides are a class of well-known reducing agents for the reduction of various metal salts to metal nanoparticles.[16−19] Specifically, a borohydride derivative, such as superhydride, $LiBEt_3H$, is easily dissolved in organic ether solvent, facilitating homogeneous reduction of metal salt and formation of metal nanoparticles.[20−23] The advantages of choosing $LiBEt_3H$ over other metal borohydrides are as follows: (i) The Li^+ cation from the superhydride can combine with Cl^- or $acac^-$ from $FeCl_2$ and $Pt(acac)_2$ to form Li salt that is easily washed off from the product with alcohol; (ii) After reduction, BEt_3 is usually released from the mixture: it may be removed from the system under nitrogen, or it can combine with other organic ether/amine/alcohol species in the mixture, to form organic adducts, leading to pure FePt nanoparticles.

The binary FePt nanoparticles are stabilized by oleic acid and oleylamine as in the previous decomposition/reduction process. If the final product is Fe-rich, then a combination of oleic acid/oleylamine in a ratio of >1 is needed for particle stabilization during the purification process. If the final product is Pt-rich, then a combination of oleic acid/oleylamine with the ratio of <1 is required for the stabilization. This corresponds to the fact that Fe tends to bind to −OOC while Pt to $-NH_2$.

Under the current reaction condition, the particle growth is self-limited. The size of the particles is independent of the amount of stabilizers present, the addition rate of reducing agent, the reduction temperature (from 200 °C to 263 °C), and the refluxing time (from 30 min to 2 h). 4 nm FePt particles were always separated. Refluxing may not be necessary, but it did help to yield FePt nanoparticles with better shape. Figure 2 shows the TEM image of 4 nm FePt nanoparticles deposited on an amorphous carbon copper grid from their hexane dispersion. It can be seen that FePt nanoparticles are uniform with narrow size distribution.

Elemental Analysis. Fe and Pt elemental analysis of the FePt powder sample shows that the mixture of 0.75 mmol of $FeCl_2$ and 0.5 mmol $Pt(acac)_2$ yielded $Fe_{60}Pt_{40}$. Similarly, 0.70 mmol of $FeCl_2$ and 0.5 mmol $Pt(acac)_2$ led to $Fe_{58}Pt_{42}$, and 0.5 mmol of $FeCl_2$ and 0.5 mmol $Pt(acac)_2$ to $Fe_{50}Pt_{50}$. Within ICP detection limit, these FePt composition data match exactly with those from the calculated ones according to the molar ratio of two metal precursors. RBS on self-assembled FePt thin films also confirmed that each kind of FePt nanoparticles has the composition close to the calculated one. For example, RBS analyses on different assemblies of $Fe_{60}Pt_{40}$ nanoparticles would usually result in ratios of $Fe_{(59-61)}Pt_{(41-39)}$. These compositional analyses of FePt nanoparticles indicate that, in this reduction method, the initial metal molar ratio is carried over to the final product, and the FePt composition is easily controlled.

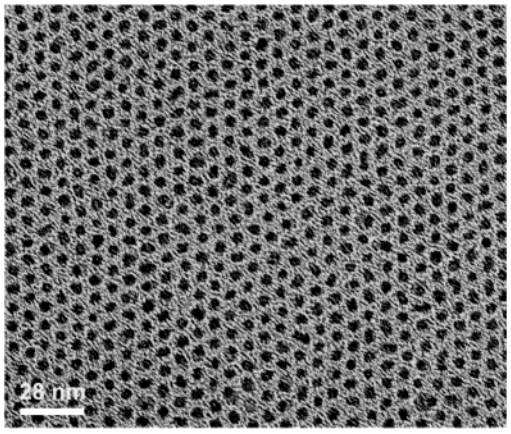

Figure 2. Bright field TEM image of a 2-D array of 4 nm FePt nanoparticles. The assembly was obtained with depositing hexane dispersion of FePt nanoparticles on an amorphous carbon coated copper grid and evaporating hexane at room temperature.

Polymer Mediated FePt Nanoparticle Assembly. The oleic acid/oleylamine coated FePt nanoparticles can be readily dispersed into hexane or chloroform solvent, facilitating surface ligand exchange and controlled nanoparticle assembly. The ligand exchange experiments show that various functional polymers can replace oleic acid/oleylamine around these nanoparticles to give polymer nanoparticle composites. For example, mixing a chloroform solution of polyethylenimine (PEI) with a hexane dispersion of FePt led to the PEI−FePt nanocomposite that is not soluble in hexane. By exchanging the stabilizers bound to the particles with multifunctional polymers that attach to a substrate, the polymer and FePt nanoparticles can be alternately adsorbed onto the substrate, and an FePt assembly with controlled thickness can be made. This polymeric molecule-assisted nanoparticle assembly is a well-known technique to produce polymer nanoparticle nanocomposites.[24−32] A densely packed self-assembled polymeric monolayer is usually obtained by spontaneous adsorption of surfactant molecules from organic solution onto a solid substrate via hydrogen bonding, ionic bonding, or covalent bonding. PEI has been found to be adsorbed on a HO-terminated substrate and is often used for gold or silica particle assembly on mica, silicon oxide and glass surfaces.[33,34] The assembly of FePt nanoparticles into a macroscopic two-dimensional array on a PEI-functionalized substrate is depicted in Figure 3A.[35] The assembly process includes (1) surface functionalization with a layer of PEI coating and (2) replacement of the particle stabilizers with a pendant functional −NH− group of the PEI. The pendant functional group −NH− extends out in the solution. By dipping the PEI-derivative substrate into the particle dispersion, ligand exchange at the PEI surface occurs and a monolayer FePt particle assembly is formed. Figure 3B shows a TEM image of one layer of 4 nm $Fe_{58}Pt_{42}$. By repeating this simple two-step process in a cyclic fashion, a PEI/FePt multilayer assembly can be obtained. Figure 3C shows a TEM image of 3 layers of 4 nm $Fe_{58}Pt_{42}$ nanoparticles self-assembled on a PEI-modified silicon oxide surface. Further experiments show this PEI-mediated assembly can be made on virtually any size and shaped HO-terminated substrates.

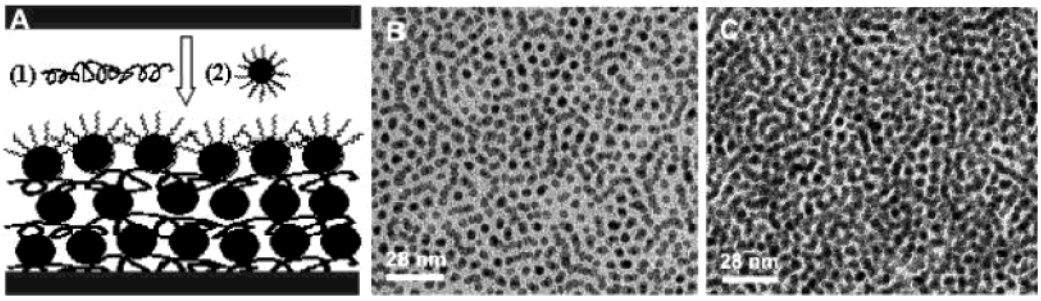

Figure 3. (A) Schematic illustration of polymer-mediated self-assembly of FePt nanoparticles by alternately adsorbing a layer of polymer (PEI) and a layer of nanoparticles on a solid surface; and TEM images of PEI-mediated assembly of 4 nm $Fe_{58}Pt_{42}$ nanoparticles on silicon oxide coated copper grids. (B) One layer assembly and (C) three layer assembly.

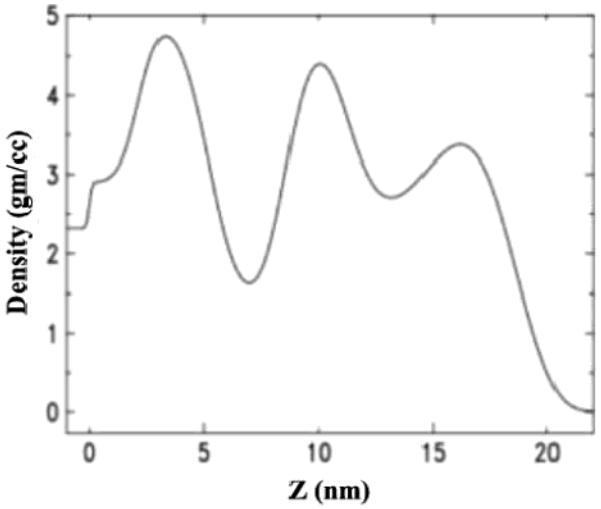

Figure 4. Mass density of a 3-layer FePt assembly, deduced from the X-ray reflectivity measurement, as a function of position from the silicon substrate (z). The silicon surface is arbitrarily defined as $z = 0$.

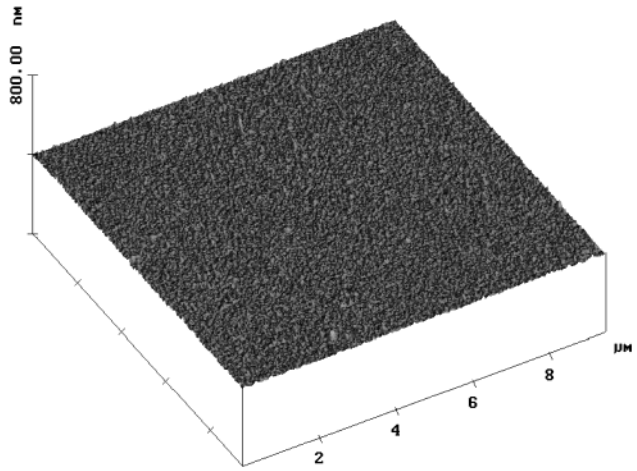

Figure 5. AFM image (9.4 × 9.4 μm^2) of a 3-layer 4 nm $Fe_{58}Pt_{42}$ nanoparticle assembly annealed at 550 °C under Ar + H_2 (5%) for 30 min.

General Analysis of the Assemblies. For a series of 2-, 3-, and 5-layered FePt nanoparticle assemblies, the depth profiling of both Fe and Pt obtained from RBS measurements is consistent with that predicted from the actual number of layers of FePt nanoparticles. The sample contains Fe, Pt, and other C, O, and N components. The overall coating thickness for a 3-layer 4 nm FePt assembly is estimated to be in the region of 10−15 nm, depending on the density and H content (not determined). The layered structure is further characterized by X-ray reflectivity analysis of nanoparticle assemblies. In X-ray reflectivity, the reflected X-ray intensity is measured as a function of incidence angle and the data are analyzed using a multilayer model that incorporates several parameters which are varied to produce the best fit to the data.[36] X-ray reflectivity measures the electron density of the nanoparticle assembly, which can be converted into mass density. The result of this analysis for a 3-layer assembly is shown in Figure 4, which plots mass density as a function of position from the silicon substrate surface. The three layers are readily evident as regions of larger mass density than the PEI between the nanoparticle layers. The spacings between the first−second and second−third layers are both 6.5 nm. These data demonstrate the layering associated with the nanoparticle assembly. Atomic force microscopy (AFM) analyses of various 3-layer thin assemblies indicate a smooth assembly surface. Figure 5 is the AFM image of a 3-layer $Fe_{58}Pt_{42}$ assembly annealed at 550 °C for 30 min on a microslide substrate. The root-mean-square (RMS) variation in height over areas of 9.4 × 9.4 μm is at 3.1 nm, which is comparable to disk height variations of the conventional recording media.

Chemical Analysis of the Assemblies. The chemical nature of the annealed films was studied using near edge X-ray absorption fine structure (NEXAFS) spectroscopy.[37] Tunable photons from a synchrotron radiation beamline can be used to study the X-ray absorption of a material as a function of photon energy. The X-ray absorption spectrum is element specific and the fine structure of the absorption edges reflects the bonding environment of the element in the compound.[37] NEXAFS data of Fe absorption on the annealed thin FePt nanoparticle assemblies indicate that all assemblies contain both metallic iron and iron oxide.[38] The iron/iron oxide fraction varies for different assemblies and depends on the FePt particle assembly thickness and annealing history of the assembly. More metallic Fe exists in a thicker assembly. For the assemblies with the same thickness, more metallic Fe is found in the assembly annealed at higher temperature or for longer time. Figure 6 shows NEXAFS spectra of the Fe L_3 and L_2 absorption edges of the 3-layers assemblies annealed at 725 °C in He atmosphere for various durations together with reference spectra of metallic Fe and Fe_3O_4. It shows that with increasing annealing duration (Figure 6A−C) the peaks corresponding to metallic Fe are increased while those to iron oxide are decreased, indicating more metallic iron is present in the assembly. Simulation based on the superposition of Fe and Fe_3O_4 (Figure 6D,E) can fit well to the observed spectra. For example, the observed spectrum for the 120 min annealed assembly (Figure 6C) corresponds to a superposition of 75%Fe/25%Fe_3O_4.[39] Assuming the particle consists of an FePt core and an oxide shell and using typical literature values for the electron escape depth for carbon (10 nm), metal (1.5 nm), and metal oxides (5 nm),[37,40] we can estimate that the relative 75%Fe/25%Fe_3O_4 contribution to the

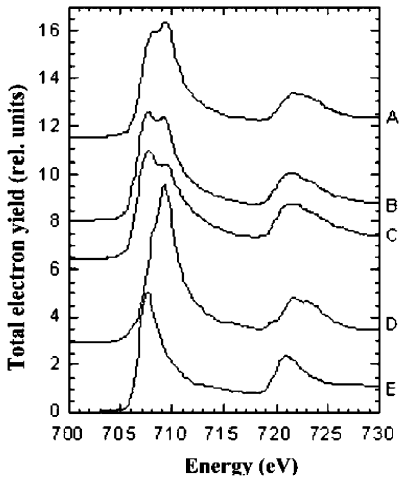

Figure 6. NEXAFS spectra of the Fe L_3 and L_2 absorption edges of 3-layer $Fe_{58}Pt_{42}$ assemblies annealed in He for various durations: (A) 2, (B) 20, and (C) 120 min, and of the reference thin films of (D) Fe_3O_4 and (E) metallic Fe.

spectrum comes from a particle with an average 0.1 nm thick oxide shell and a 3.8 nm metallic particle core. Although the accurate electron escape depths in our sample are not available, preventing us from getting the exact value for the iron/iron oxide fraction, the estimate shows that a very thin oxide shell is indeed present in the assemblies. The chemical origin of the iron oxide is easily understood considering the fact that both the decomposition of the iron oleate on an FePt particle surface during the annealing and air oxidation of the surface iron atom of an annealed FePt particle will both lead to iron oxide.

Structural Analysis of the Assemblies. The crystal structure of the FePt nanoparticles in a thin assembly was determined by the X-ray diffraction (XRD). The XRD of the as-synthesized FePt particles reveals a typical chemically disordered fcc structure,[8] in which Fe atoms are substituted into Pt positions and vice versa. Annealing induces the Fe and Pt atoms to rearrange into the long range chemically ordered fct structure, which can be viewed as a natural superlattice of alternating Fe and Pt atomic planes. The change of the internal particle structure upon annealing depends on annealing temperature and duration, as well as the Fe/Pt ratio. The onset of this phase change occurs at about 500 °C, which is consistent with the previous observation on FePt nanoparticles prepared from the decomposition/reduction process.[8,41,42] Figure 7 shows the in-plane X-ray diffraction scans for the as-synthesized 3-layer $Fe_{58}Pt_{42}$ assembly (Figure 7A) and for the one annealed for 2 min at 725 °C in He atmosphere (Figure 7B). Figure 7B shows the typical superlattice peaks of (001) and (110) that are characteristic of the ordered FePt ($L1_0$) compound phase.[6] The one-dimensional chemical ordering parameters S can be obtained from the ratio of the peak intensity of the superlattice peaks to the fundamental peaks.[43] S is unity for perfectly ordered films and is zero for a chemically disordered film. This order parameter depends on the annealing history of the sample. Figure 8A illustrates the increase of the S with annealing time at 725 °C. It shows that for the as synthesized assembly the order parameter is zero and is increased up to almost 1 for the sample annealed for 2 h duration. The order parameter also varies with annealing temperature at the same annealing time. It increases with temperature from 0.6 at 500 °C for 5 min to 0.8 at 800 °C for 5 min.

Annealing Induced Particle Aggregation. High temperature annealing also leads to particle aggregation. Previous in situ

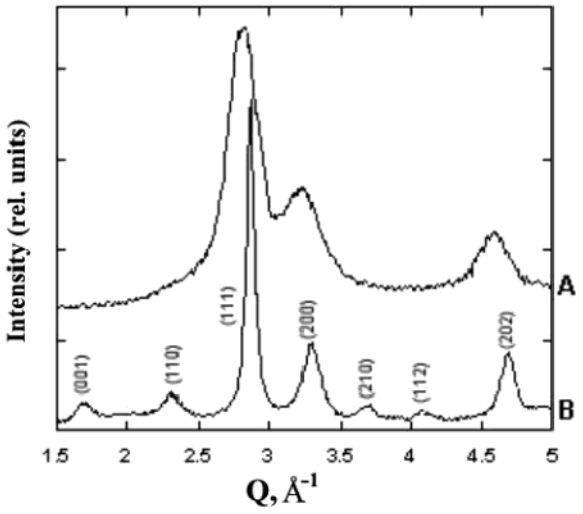

Figure 7. XRD scans of 3-layer $Fe_{58}Pt_{42}$ assemblies. (A) As-synthesized 3-layer assembly and (B) 3-layer assembly annealed at 725 °C for 2 min in He atmosphere, in which the diffraction peaks are indexed following the fct structure.

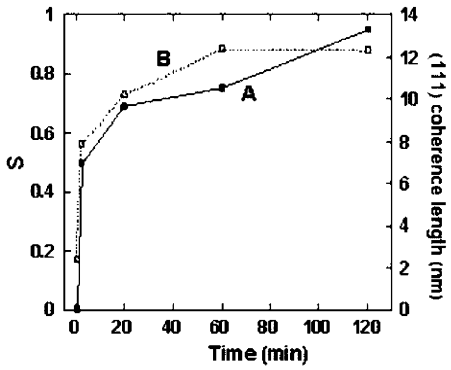

Figure 8. (A) Fe, Pt order parameter, S and (B) (111) coherence length of the FePt particles as a function of annealing duration. The data were extracted from the XRD scans of the 3-layer $Fe_{58}Pt_{42}$ nanoparticle assemblies annealed in He at 725 °C.

TEM experiments have clearly shown coalescence of FePt particles annealed at 600 °C under high vacuum for 1 h.[42] From the line width of the (111) peak, it is also possible to estimate the (111) coherence length that is related to the particle diameter.[44] Figure 8B shows the (111) coherence length vs annealing time at annealing temperature 725 °C. For the 2 min annealed assembly, the coherence length has increased from 2.8 nm for the as synthesized assembly to 8 nm, and it increases further with annealing duration. The average particle size increases also with annealing temperature. The particle size estimated from XRD line width for 3-layer assemblies annealed at 580 °C for 30 min is 5 nm but rises to 17 nm for a 800 °C/5 min annealed sample. To prevent agglomeration of the FePt nanoparticles, ion beam irradiation of the as-synthesized 4 nm FePt nanoparticle assemblies with the goal of hardening the carbonaceous binder that separates the nanoparticles was applied to treat the thin assembly. The irradiation was performed on as synthesized nanoparticles deposited on naturally oxidized Si (100) wafers, using 2 MeV He^+ ions at a dose of 2×10^{16} ions per square centimeter. The samples were cooled during processing at room temperature. Our preliminary experiments showed that, although the ion beam did not transform the organic coating into diamond-like carbon, it did reduce agglomeration of FePt nanoparticles during subsequent high-temperature annealing.

Magnetic Properties of the Assemblies. Along with the structural change, magnetic properties of the assemblies can be

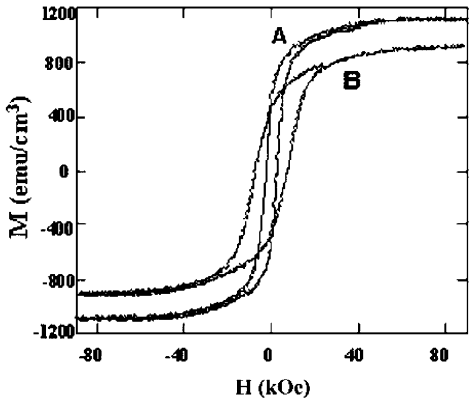

Figure 9. In-plane hysteresis loops of 3-layer $Fe_{58}Pt_{42}$ nanoparticle assemblies annealed for (A) 2 min and (B) 20 min in He at 725 °C. The loops were measured by VSM at room temperature.

easily tuned. The as-synthesized FePt nanoparticles have chemically disordered fcc structure, and the related thin assemblies are superparamagnetic at room temperature with $H_c = 0$. The thermal annealing transforms the chemically disordered fcc structure to the chemically ordered fct structure, yielding ferromagnetic thin FePt nanoparticle assemblies. The coercivity of the annealed thin films increases with annealing time and temperature, and a minimum annealing temperature of about 500 °C under an inert atmosphere is required to form ferromagnetic thin films. This corresponds to the structure transformation from the fcc phase to the fct phase at this temperature. On the other hand, the coercivity of the annealed thin films is also found to depend on the assembly thickness. This is likely due to the variation of the net iron/iron oxide ratio with the assembly thickness, as observed using NEXAFS. Figure 9 shows the room-temperature hysteresis loops of two 3-layer 4 nm $Fe_{58}Pt_{42}$ nanoparticle assemblies annealed in He at 725 °C for different time. Figure 9A is the loop from 2 min annealed sample, whereas Figure 9B is the loop from 20 min annealed sample. The moment density is normalized to the nanoparticle volumes assuming a packing density of 0.13 that can be estimated from the TEM measurements (Figure 3C). The 2 min annealed sample has a moment density that is comparable to thin film and bulk FePt of 1140 emu/cm^3,[2] its coercivity is 2400 Oe. For the 20 min annealed sample, the estimated moment density is slightly lower than that from the 2 min annealed sample, at 930 emu/cm^3, but the coercivity is greatly increased to 7600 Oe, indicating better chemical ordering of Fe and Pt in the longer time annealed sample. This is consistent with FePt ordering parameter increase with annealing time indicated in Figure 8A. Different from the annealed sample, the unannealed sample shows a very low moment density of about 45 emu/cm^3 at room temperature due most likely to superparamagnetism of the particles and a higher percentage of iron oxide in the assembly.

Magnetic properties of the thin FePt nanoparticle assemblies can be further improved by annealing the assembly under Ar + 5%H_2 as the reducing atmosphere can reduce the iron oxide layer present around each FePt nanoparticle. Magnetic measurements show that a 3-layer $Fe_{58}Pt_{42}$ assembly annealed at 450 °C is ferromagnetic with coercivity reaching 800 Oe. Annealing at 700 °C can yield an assembly with coercivity of over 1 T. However, high-temperature annealing also results in serious particle aggregation and exchange-coupling among the neighboring particles.[45] Further experiments on controlled reductive annealing and its application in fabricating thin FePt assemblies with large H_c are underway.

Conclusions

We have reported that superhydride reduction of $FeCl_2$ and $Pt(acac)_2$ in the presence of oleic acid, oleylamine, and 1,2-hexadecanediol can be used to make 4 nm FePt nanoparticles. The initial molar ratio of two metal precursors is carried over to the final product, and the composition of final FePt is easily tuned. Alternately, absorbing a layer of polyethylenimine and the FePt nanoparticles onto a solid substrate results in FePt nanoparticle assemblies with tunable thickness. Thermal annealing induces the internal particle structure from chemically disordered fcc to chemically ordered fct and transforms the thin assembly from superparamagnetic to ferromagnetic. The reported synthesis and assembly of FePt nanoparticles offers a convenient process of fabricating FePt nanoparticle based functional devices that may be suitable for various magnetic applications.

Acknowledgment. We thank A. J. Kellock for RBS measurements.

References and Notes

(1) Weller, D.; Moser, A. *IEEE Trans. Magn.* **1999**, *35*, 4423.
(2) Weller, D.; et al. *IEEE Trans. Magn*. **2000**, *36*, 10.
(3) Liu, S. H. *IEEE Trans. Magn*. **1999**, *35*, 3989.
(4) Sqalli, Q.; Brenal, M. P.; Hoffmann, P.; Marquis-Weible, F. *Appl. Phys. Lett.* **2000**, *76*, 2134.
(5) Kneller, E. F.; Hawig, R. *IEEE Trans. Magn*. **1991**, *27*, 3588.
(6) Farrow, R. F. C.; et al. *J. Appl. Phys.* **1996**, *79*, 5967.
(7) Moser, A.; et al. *J. Phys. D: Appl. Phys.* **2002**, *35*, R157.
(8) Sun, S.; Murray, C. B.; Weller, D.; Folks, L.; Moser, A. *Science* **2000**, *287*, 1989.
(9) Sun, S.; Fullerton, E. E.; Weller, D.; Murray, C. B. *IEEE Trans. Magn*. **2001**, *37*, 1239.
(10) Harrell, J. W.; Wang, S.; Nikles, D. E.; Chen, M. *Appl. Phys. Lett*. **2001**, *79*, 4393.
(11) Stahl, B.; et al. *Adv. Mater*. **2002**, *14*, 24.
(12) Li, Y.; Liu, J.; Wang, Y.; Wang, Z. L. *Chem. Mater.* **2001**, *13*, 1008.
(13) Chen, M.; Nikles, D. E. *Nano Lett*. **2002**, *2*, 211.
(14) Kang, S.; Harrell, J. W.; Nikles, D. E. *Nano Lett.* **2002**, *2*, 1033.
(15) Wood, R. *IEEE Trans. Magn*. **2000**, *36*, 36.
(16) Schlesinger, H. I.; et al. *J. Am. Chem. Soc.***1953**, *84*, 1493.
(17) Yiping, L.; Hadjipanayis, G. C.; Sorensen, C. M.; Klabunde, K. J. *J. Magn. Mag. Mater*. **1989**, *79*, 321.
(18) Glavee, G. N.; Klabunde, K. J.; Sorensen, C. M.; Hadjipanayis, G. C. *Langmuir* **1994**, *10*, 4726.
(19) Sun, Y.-P.; Rollins, H. W.; Guduru, R. *Chem. Mater*. **1999**, *11*, 7.
(20) Bonnemann, H.; Brijoux, W.; Joussen, T. *Angew. Chem., Int. Ed. Engl*. **1990**, *29*, 273.
(21) Bonnemann, H.; Brinkmann, R.; Koppler, R.; Neiteler, P.; Richter, J. *Adv. Mater*. **1992**, *4*, 804.
(22) Sun, S.; Murray, C. B. *J. Appl. Phys.* **1999**, *85*, 4325.
(23) Sun, S.; Murray, C. B.; Doyle, H. *Mater. Res. Soc. Symp. Proc*. **1999**, *577*, 385.
(24) Fendler, J. H. *Chem. Mater*. **1996**, *8*, 1616.
(25) Liu, Y.; Wang, A.; Claus, R. *J. Phys. Chem. B* **1997**, *101*, 1385.
(26) Cassagneau, T.; Mallouk, T. E.; Fendler, J. H. *J. Am. Chem. Soc*. **1998**, *120*, 7848.
(27) Aliev, F. G.; et al. *Adv. Mater*. **1999**, *11*, 1006.
(28) Rogach, A. L.; Koktysh, D. S.; Harrison, M.; Kotov, N. A. *Chem. Mater*. **2000**, *12*, 1526.
(29) Halaoui, L. I. *Langmuir* **2001**, *17*, 7130.
(30) Kotov, N. A. *MRS Bull.* **2001**, 992.
(31) Lvov, Y. M.; Price, R. R. *Colloid Surf. B: Biointerfaces* **2002**, *23*, 251.
(32) Hicks, J. F.; Seok-Shon, Y.; Murray, R. W. *Langmuir* **2002**, *18*, 2288.
(33) Schmitt, J.; Mächtle, P.; Eck, D.; Möhwald, H.; Helm, C. A. *Langmuir* **1999**, *15*, 3256.
(34) Hua, F.; Cui, T.; Lvov, Y. *Langmuir* **2002**, *18*, 6712.
(35) Sun, S.; et al. *J. Am. Chem. Soc.* **2002**, *124*, 2884.
(36) Holy, V.; Pietsch, U.; Baumbach, T. *High-Resolution X-ray Scattering from Thin Films and Multilayers*; Springer-Verlag: Berlin, 1998.
(37) Stöhr, J. *NEXAFS Spectroscopy*; Springer: Berlin, 1992.
(38) Anders, S.; et al. *Microelectron. Eng.* **2002**, *61/62*, 569.

(39) Other forms of iron oxide, such as Fe_2O_3, may also exist in the assembly. Because of the surface sensitivity of NEXAFS and the similarity of iron oxide spectra, the exact nature of iron oxide in the assembly is difficult to determine.

(40) Regan, T. J.; et al. *Phys. Rev. B* **2001**, *64*, 214422.

(41) Weller, D.; Sun, S.; Murray, C. B.; Folks, L.; Moser, M. *IEEE Trans. Magn*. **2001**, *37*, 2185.

(42) Dai, Z. R.; Sun, S.; Wang, Z. L. *Nano Lett.* **2001**, *1*, 443.

(43) Cebollada, A.; Farrow, R. F. C.; Toney, M. F. In *Magnetic Nanostructures*; Nalwa, H. S., Ed.; American Scientific Publishers: Stevenson Ranch, CA, 2002; p 93.

(44) Klug, H. P.; Alexander, L. E. *X-ray diffraction Procedures for Polycrystalline and Amorphous Materials*; John Wiley & Sons: New York, 1962; pp 491−538.

(45) Zeng, H.; Sun, S.; Vedantam, T. S.; Liu, J. P.; Dai, Z. R.; Wang, Z. L. *Appl. Phys. Lett.* **2002**, *80*, 2583.